3

Event-triggered Sliding Mode Control for a pre-regulator PFC stage

In previous Chapter, the concept of Event-triggered Sliding Mode Control (ETSMC) was applied to DC-DC stage of the two-stage AC-DC-DC converter of an electronic equipment, required for voltage regulation and isolation. The concept was explained and analysed, in detail. In this Chapter, the scheme is extended to PFC stage of the two-stage AC-DC-DC converter used at the front end of an electronic equipment.

Electronic equipment, ranging from battery chargers to computers, use a full-bridge rectifier for AC to DC conversion. The front-end rectification is carried out in order to convert utility AC into workable DC. The process, in turn, distorts the current drawn from the grid. In the present scenario, the number of such non-linear loads, getting connected to the grid, is increasing exponentially. The electronic market is amongst the largest and fastest growing manufacturing industry across the globe, with computer systems and consumer electronics making about 40% of the total production [NITIAayog, 2016]. These appliances do not disrupt the power quality much, individually. However, their cumulative effect is severe as presented in [Timens *et al.*, 2011]. This increase in number of loads, has increased the probability of distorting the AC supply waveform. Taking cognizance of this fact many countries have started to impose regulatory measures like IEC 61000-3-2 Harmonics Standards by the European Union for these type of devices [IECLimits, 2014].

The aforementioned regulation classifies the equipment, working with input power exceeding 75 W, in four classes viz. A, B, C, and D. Portable equipment make it to Class B, while Class C is for lighting equipment, and whole Class D is just for TV sets, monitors, and computer peripherals. Rest all of the devices qualify as Class A equipment. The classification of appliances is presented in Table 3.1.

Table 3.1 : Classification of Equipment According to IEC610000-3-2 (2014)

Class	Equipment
Class A	Balanced three phase equipment
	Household appliances excluding those identified as Class D
	Tools excluding portable tools
	Dimmers for incandescent lights
	Audio equipment
	Everything else which is not classified as Class B, C or D.
Class B	Portable tools
	Arc welding equipment which is not a professional equipment
Class C	Lighting equipment
Class D	Personal computers and monitors
	Television receivers

The regulatory bodies have laid down some rules to keep this distortion in check. The mea-

sure of this distortion is given in terms of permissible harmonic current for each harmonic order. Amongst all the classes the regulatory limits are the strictest for Class D. Therefore, if the measured current harmonics of any equipment (irrespective of the class) falls within these limits then the system will surely comply with the regulation. The harmonic limits for Class D equipments is presented in Table 3.2.

Table 3.2 : Harmonic limits for Class D equipments

Harmonic Order (n)	**Maximum Permissible Harmonic Current per Watt (mA/W)**	**Maximum Permissible Harmonic Current (A)**
3	3.4	2.30
5	1.9	1.14
7	1.0	0.77
9	0.5	0.40
11	0.35	0.33
13	0.29	0.21
$15 \leq n \leq 39$ (only odd harmonics)	$\frac{3.85}{n}$	$0.15\frac{15}{n}$

Thereby, Power factor correction converters are finding their place in all modern electric equipment now. The literature provides a plethora of power factor correction converters to make the current waveform meet the regulatory standards [Garcia *et al.*, 2003; Pereira *et al.*, 2015; Qiao and Smedley, 2001; Singh *et al.*, 2011]. It involves high frequency switching converters, operated using suitable controller, to shape the input current. Fundamental principle behind PFC is to make the circuit behave as a pure resistor. The notion of Loss-free resistor (LFR), discussed later in the Chapter, therefore, makes for an ideal and natural choice in power factor application [Bist and Singh, 2015; Cid-Pastor *et al.*, 2013; Flores-Bahamonde *et al.*, 2014; Haroun *et al.*, 2014; Marcos-Pastor *et al.*, 2015; Nasirian *et al.*, 2013; Singer *et al.*, 2004].

The regulatory bodies, however, do not demand a unity power factor, the regulations are imposed to keep the harmonic current amplitudes, at all load levels, in check. Thereby, a little flexibility in wave shaping can be leveraged, and the current envelope can deviate from the reference wave as long as it stays within the boundary. That is exactly the working principle of Hysteresis modulation (HM) control and therefore this is widely accepted control technique for this application. However, for HM the boundary layer stays fixed for all load conditions, which means, even though the load has changed, the tolerance band for the current stays fixed. More so, it is to be noted that the allowable harmonic current is given in terms of mA/W, implying the permissible harmonic content is load dependent. The fixed band at all loads for this case would mean that the deviation of the current is restricted below the permissible limits leading to unnecessary switching. This suggests for the band to change its size with the load conditions. Thus the concept of Event-triggered SMC makes an inherent choice of control.

In this Chapter, a pre-regulator PFC stage in single-phase circuits is adopted. Input current of the system is made to follow the input voltage, in shape, using the sliding mode based LFR [Cid-Pastor *et al.*, 2013]. The adopted work is then implemented, on a boost PFC converter, following the event-based strategy. The organisation of the Chapter is as follows: In Section 3.1 the background of non-linear loads is presented. Section 3.2 gives the preliminaries of Loss-free resistor. In Section 3.3 Sliding mode based Loss-free resistor (SLFR) is presented and analysed. Event-triggered SLFR is proposed in Section 3.4. Simulation results and experimental validation is presented in Section 3.5. Section 3.6 summarizes the Chapter.

3.1 BACKGROUND OF NON-LINEAR LOADS

Generally, any device requiring AC/DC rectification, presents itself as a non-linear load to the mains. The basic circuit configuration involves typical rectifier at the front end of a switch mode power supply. This circuit has a reservoir capacitor at its output. The load draws current only when the input voltage is more than the capacitor voltage. This current then charges the capacitor. As the input voltage from the rectifier falls, the capacitor supplies to the output load. Thereby, the load draws a pulsating type of current from the supply instead of a well-distributed sinusoidal current.

In order to comprehend this, Fig.3.1 shows experimental plots of a single-stage boost PFC converter for (a) uncompensated and (b) compensated system. Here, the uncompensated system represents the open loop system without any control whereas, the compensated system represents the single-stage boost PFC controlled using proposed controller. In Fig.3.1, V_{in} is the input supply voltage, I_{in} is the input current of the converter, and V_o is output load voltage. V_{in} is a 100 V, 50 Hz sinusoidal AC voltage. The uncompensated system exhibits the open loop performance of the PFC converter to a pulse of 0.2 duty cycle and switching frequency 25 kHz. As seen the input current shows a pulsating behaviour and the supply voltage wave also gets flattened around the top. The compensated system is the converter controlled using proposed method. The resultant waveform follows the supply voltage and is of high power factor.

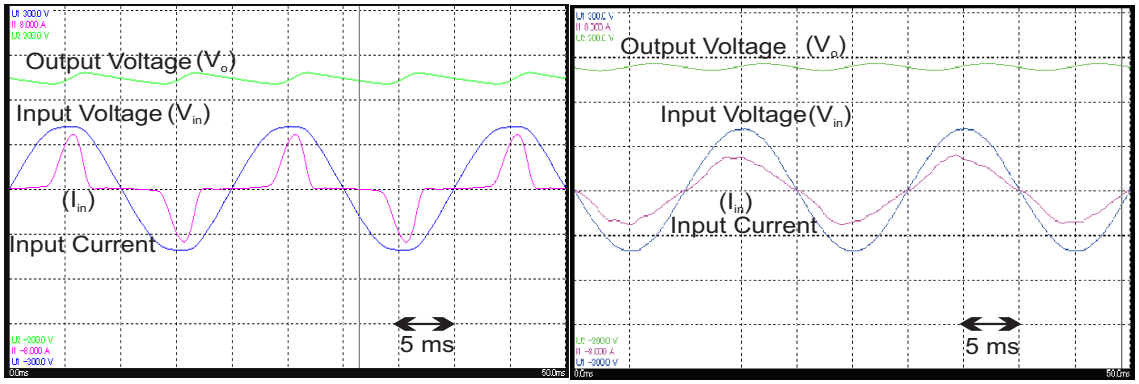

Uncompensated System

Compensated System using proposed controller

Figure 3.1 : (a) Uncompensated (b) Compensated

3.2 PRELIMINARIES OF LOSS-FREE RESISTOR

Resistive elements form a vital part of the power processing applications to serve purposes like damping of the electromechanical and mechanical vibrations, curbing the oscillatory waveform (ringing) in switched systems, compensating for negative resistance to achieve stable operation, to name a few. However, incorporating traditional resistive elements in the system comes at a price of high losses and hence, reduced efficiency. Thereby, the need to develop an efficient, loss-less system has motivated the notion of loss-free resistor (LFR) by Singer (see [Singer *et al.*, 2004] and the references therein).

Initially, the concept was confined to the acknowledgement that certain switching converters like buck-boost, Ćuk, SEPIC etc., working in DCM, display inherent property of being resistive at the input. Later, the notion evolved from relying on the DCM operation to using feedback controllers to attain switching converter with resistive input impedance. Apart from PFC, this concept of LFR, either inherent or enforced, has been borrowed for various practices which earlier had to

resort to using traditional resistances. The applications involve DC impedance matching for MPPT [Haroun *et al.*, 2015], LED driver [Lamar *et al.*, 2015], realizing sources with loss-free characteristics [Wang *et al.*, 2001], energy harvesting application [Wang *et al.*, 2013a] to name a few.

As described in the work [Singer *et al.*, 2004], an ideal LFR is a two-port switching structure which satisfies two basic conditions of current proportionality and power balance.

- The input current is following the input voltage.
  $V_1 = rI_1$
- The input power absorbed is completely fed to the output. $V_1 I_1 = V_2 I_2$

Where, V_1, I_1, V_2, and I_2 are the rms equilibrium values of the instantaneous variables shown in Fig. 3.2. The proportionality constant r is the emulated input resistive impedance, under steady state.

A circuit of LFR as two-port network is shown in Fig. 3.2.

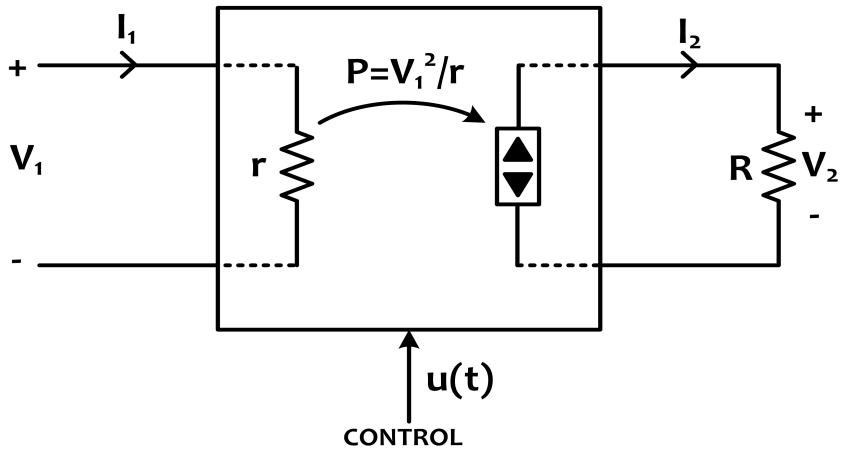

Figure 3.2 : A circuit of LFR as a two-port network.

3.3 SLIDING MODE BASED LOSS-FREE RESISTOR (SLFR)

The authors in [Cid-Pastor *et al.*, 2013], have proposed a seminal work on boost based SLFR for shaping the input current so that it follows the input voltage. The system under consideration is depicted in Fig. 3.3.

The bridge rectifier is fed by a sinusoidal AC voltage. At the output of which, a boost converter is connected. The converter dynamics can be represented mathematically using state-space averaging as:

$$\dot{x_1} = \frac{-x_2}{L_o}(1-u) + \frac{v_1}{L_o} \tag{3.1a}$$

$$\dot{x_2} = \frac{x_1}{C_o}(1-u) + \frac{-x_2}{RC_o} \tag{3.1b}$$

Where, x_1 and x_2 are the states of the system representing Inductor Current and Output Voltage respectively. u is the control input. v_1 is the rectified input voltage and L_o, C_o, and R are the inductance, capacitance and load resistance respectively.

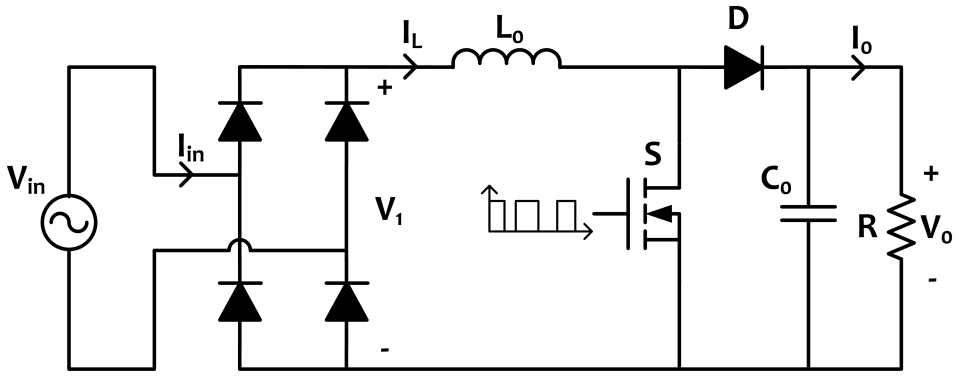

Figure 3.3 : PFC based on a boost converter

The above Boost converter is controlled using a classical SMC. Design of Sliding Mode Control to realize LFR involves the following two design steps,

- Selection of switching surface on which motion should be restricted, and
- Synthesis of a control law which makes the selected surface attractive. This condition is also called existence condition.

3.3.1 Switching function

The switching function for the Sliding mode control (SMC) [Utkin *et al.*, 1999] adopted for PFC application is defined as:

$$s(x,t) = x_1 - x_{1ref} \tag{3.2}$$

Where, x_1 is a linear combination of state variables which form the input current. Since the current must follow the voltage, the reference current term x_{1ref} is replaced by $g(t)v_1$. Where, v_1 is the rectified input voltage and $g(t)$ is the proportionality constant equal to the inverse of the emulated input impedance $r(t)$ [Marcos-Pastor *et al.*, 2015].

3.3.2 Control Law

The control law must be chosen such that it drives the system trajectories, from any initial point, to the switching surface. The transversality condition evaluates the capability of the control input to modify the system behaviour in the desired manner. It needs

$$\frac{d}{du}(\frac{ds}{dt}) \neq 0$$

In this case, it can be seen that

$$\frac{d}{du}(\frac{ds}{dt}) = \frac{x_2}{L_o} > 0 \tag{3.3}$$

Since (3.3) is always satisfied, the transversality is positive for all the conditions. The adopted switching law must follow

$$u = \begin{cases} 0, & \text{if } s > 0. \\ 1, & \text{if } s < 0. \end{cases} \tag{3.4}$$

Therefore, the adopted control law for this application is:

$$u = \frac{1}{2}[1 - sign(s)] \tag{3.5}$$

3.3.3 Equivalent Control

From the transversality condition

$$\frac{d}{du}(\frac{ds}{dt}) \neq 0$$

Hence, the continuous equivalent of the control law (3.5) is found by

$$\frac{ds}{dt}\Big|_{u=u_{eq}} = 0$$

Using (3.1), the derivative of (3.2) is obtained for a time varying input voltage, assuming g to be constant for an operating condition, as

$$\dot{s} = \frac{-x_2}{L_o}(1-u) + \frac{v_1}{L_o} - g\frac{dv_1}{dt} \tag{3.6}$$

Replacing u by u_{eq} and equating it to 0, leads to the following expression for equivalent control.

$$u_{eq} = \frac{(\frac{x_2 - v_1}{L_o}) + g\frac{dv_1}{dt}}{\frac{x_2}{L_o}} \tag{3.7}$$

3.3.4 Ideal Sliding Dynamics Analysis

The analysis in this section has been carried out in light of the work done in [Cid-Pastor *et al.*, 2013]. When the system reaches the sliding-mode, i.e. $s = 0$ is satisfied, leading to $x_1(t) = gv_1(t)$ and therefore the corresponding system dynamics is expressed using $u = u_{eq}$ and imposing condition $s = 0$ in (3.1)

$$C_o x_2 \frac{dx_2}{dt} + \frac{{x_2}^2}{R} = x_{1ref}\{v_1 - L_o\frac{dx_{1ref}}{dt}\} \tag{3.8}$$

Here, v_1 is supplied by a rectifier and the admittance g is assumed constant, then

$$v_1 = V_p|sin(\omega t)| \tag{3.9a}$$
$$x_{1ref} = gV_p|sin(\omega t)| \tag{3.9b}$$

Therefore,

$$v_1 x_{1ref} = g{V_p}^2 sin^2(\omega t) \tag{3.10a}$$
$$L_o x_{1ref}\frac{dx_{1ref}}{dt} = \omega L_o (gV_p)^2 sin(\omega t).cos(\omega t) \tag{3.10b}$$

Substituting (3.10) in (3.8), the dynamics becomes

$$x_2\frac{dx_2}{dt} + \frac{{x_2}^2}{RC_o} = f(t) \tag{3.11}$$

Where, $f(t) = \frac{g{V_p}^2}{C_o}[sin^2(\omega t) - \omega L_o g sin(\omega t)cos(\omega t)]$

3.3.5 Analysis of System dynamics

The complete solution containing both transient and steady state responses under ideal sliding-mode dynamics is presented in this section. Let $y = \frac{x_2^2}{2}$, then (3.11) can be written as

$$\frac{dy}{dt} + 2\frac{y}{RC_o} = f(t) \tag{3.12}$$

This is a linear first order ordinary differential equation with constant coefficients whose solution is given by

$$y = \kappa e^{-2t/RC_o} + g\frac{V_p^2}{4}R[1 + ACos(2\omega t) - Bsin(2\omega t)] \tag{3.13}$$

where, $A = \frac{\omega^2 RC_o L_o g - 1}{1+(\omega RC_o)^2}$; $B = \frac{\omega RC_o + \omega L_o g}{1+(\omega RC_o)^2}$ and κ is a constant depending on initial conditions. The first term in (3.13), gives the transient response, and since, it goes to zero as time increases the system is stable. The second term is the steady state response of the system, which is written in terms of output voltage x_2 as

$$x_2 = V_p\sqrt{\frac{gR}{2}}[1 + ACos(2\omega t) - Bsin(2\omega t)]^{\frac{1}{2}} \tag{3.14}$$

From (3.14), it can be seen that the resistive load gets an average output power of $\frac{V_p^2}{2}g = \frac{v_1^2}{r}$, which is the averaged input power absorbed by the SLFR at the input port.

Thus, for an ideal switching converter, input power is equal to output power, hence making a case of *POPI* structure. Under steady state, when $s = 0$, $i_L = gV_1$ is satisfied, the input current will follow the input voltage. Hence, on account of meeting the above two specified conditions, the LFR is realized using SMC. The power balance equation of a loss-less resistive impedance gives,

$$\frac{V_1^2}{r} = \frac{V_2^2}{R} \tag{3.15}$$

therefore, the output voltage is given as

$$V_2 = V_1\sqrt{\frac{R}{r}} \tag{3.16}$$

3.4 EVENT-TRIGGERED SLFR

This section discusses the event-triggered implementation of SLFR realized in the previous section. As discussed, the IEC 61000-3-2 Harmonics Standards by European Union demand the harmonic content of the input current to be below a certain level. The fact that the harmonic current does not need to be entirely eliminated rather must be contained within the prescribed limits, has been the motivation behind adopting event-triggered implementation of SLFR. In the adopted strategy, the control is not updated continuously, and is held to its previous value till the defined triggering condition is reached. This triggering condition is defined such that it takes care of the currents following the regulations, while avoiding unnecessary switching required for perfect power factor.

The memory based triggering condition for the PFC application is

$$|e| \leq \sigma|x| \tag{3.17}$$

The error term is defined as $e = x(t_i) - x(t)$, wherein $x(t) = i_L(t)$. Until the condition (3.17) is violated, the states are not updated to their current values and hence, the control law given in (3.5), is held to its previous value. The pictorial presentation of the concept and its implementation has been given in the next subsection.

3.4.1 Event-triggered SMC for PFC

In event-triggering control, the control input is held to its previous value until the event-triggering condition $|e| \leq \sigma x$ is breached. The fulfilment of this condition marks an event. At each event, the state values get updated to their current value. This process for the PFC application is shown in Fig. 3.4.

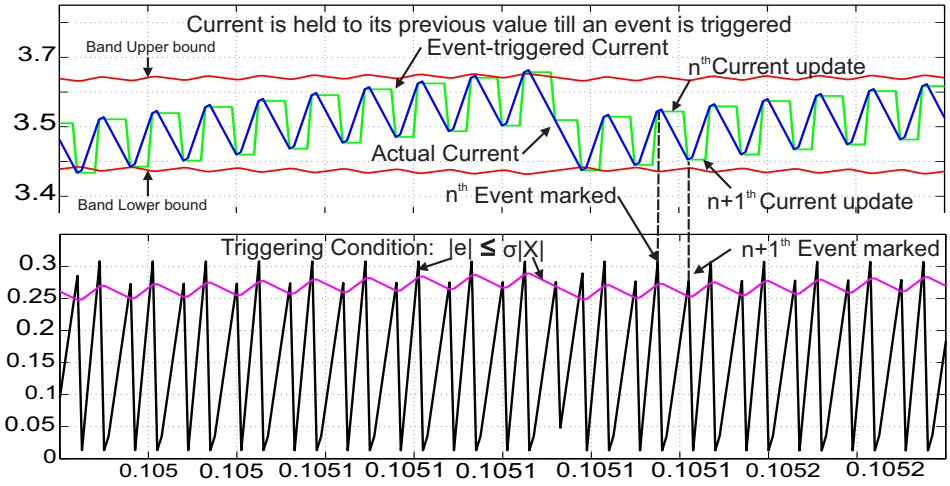

Figure 3.4 : Event-triggered SMC for PFC

The evolution of $|e|$ (in black) when crosses the $\sigma|x|$ bound (in purple), an event is marked. At this point, the event-triggered state i.e. the inductor current (in green) is updated to the corresponding value of the actual state (in blue). This asynchrony gives flexibility to the current to move away from the reference value but always within the boundary (in red). Moreover, since the control is held between the two triggering instants, the needless switching and thus, the loss associated with it, is avoided.

3.4.2 Comparison of HM-SMC and ETSMC

This section discusses the popularity of HM-SMC for PFC application and briefly presents it's working principle. Following which the need for ETSMC is established. Since the aim of PFC is to keep the harmonic distortion in limit rather than achieving perfect unity power factor, a slight deviation in the current about its reference signal is allowed. This is preferred so as to maintain the %THD within the limit but with a significant reduction in switching instances. In line with the above aim, Hysteresis modulation based SMC makes an inherent choice for this application and thereby is widely adopted. The working principle of HM-SMC is shown in Fig. 3.5

As shown, the band is fixed here and the switch changes its state whenever the current values outflows the defined boundary. HM-SMC has been established as a special case of ETSMC with memory less triggering condition, wherein the system states are not leveraged, in Chapter 2. Therefore, the boundary conditions in HM-SMC stay fixed for all load and line conditions and are usually designed for the worst case. Thereby, even when conditions are not extreme, there is significant switching to keep the current within the pre-defined band.

Another stimulating feature of the IEC regulations is that, for Class D appliances, the limits are given in terms of mA/W. This nature defines that at different load levels the permissible harmonic content varies. Hence, the allowable deviation of the current from its reference value must also vary. Therefore, the methodology of HM-SMC, involving a fixed pre-defined band at all load levels, will not serve the purpose and will cause unneeded switching actions to restrict the

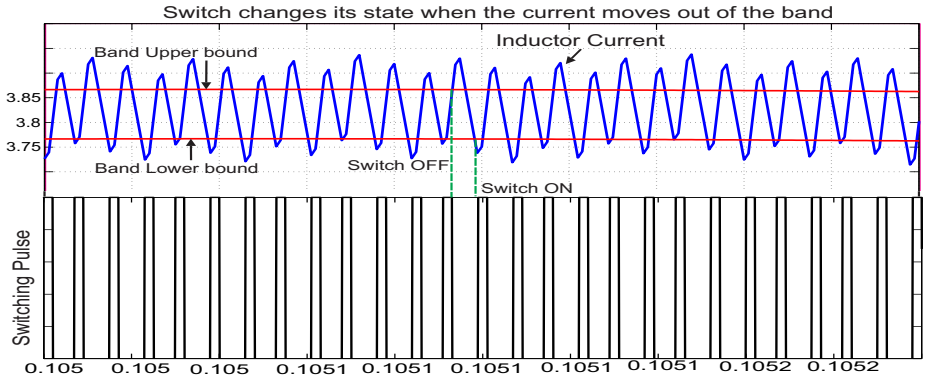

Figure 3.5 : Principle of HM-SMC

current deviations. That is why an adaptive allowable band around reference current with various load conditions is needed to allow for a flexibility in band sizes around the reference current value. Event-triggered based SLFR leverages system state to change the permissible boundary conditions and this forms the basic difference between HM-SMC and ETSMC. Results pertaining to this section is presented in the next section.

3.5 SIMULATION AND EXPERIMENTATION STUDIES

This section presents the simulation study of the proposed control scheme. The results are categorized into two subsections; first section compares the Event-triggered and Classical SMC for PFC application. In the next section, load adaptive nature of the proposed ETSMC scheme is analysed and a comparative study of the proposed scheme is carried out with the widely adopted HM-SMC control for PFC application.

3.5.1 Event-triggered vs Classical SLFR

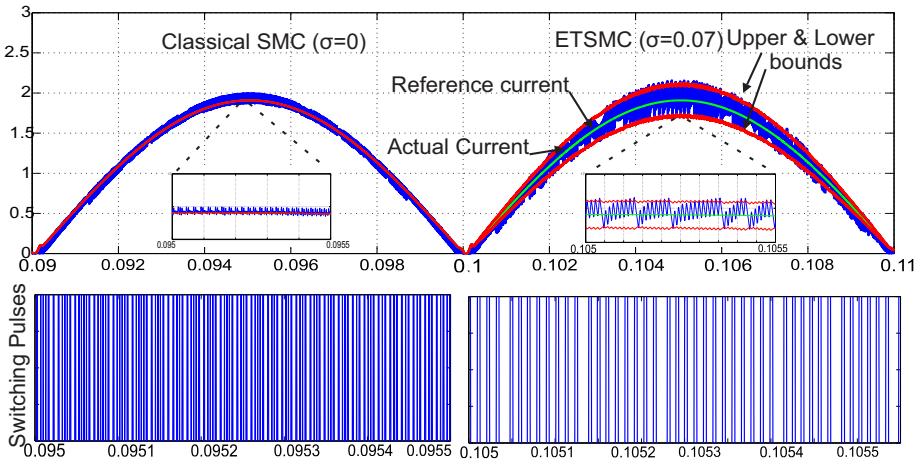

Figure 3.6 : Power factor correction for SMC and ETSMC and the corresponding switching signal

In Fig. 3.6, the power factor correction is shown for the SMC and ETSMC along with the corresponding switching pulses. For ETSMC, the actual current (in blue) is allowed to deviate from the reference current (in green), however, it will still be contained within the band marked in red. For classical SMC, since $\sigma = 0$, there is no band and the current is required to follow the

reference signal strictly. The zoom-in and the pulses corresponding to that section is also shown in the figure. As seen, there is a significant difference between the switching pulse density for the two cases. The %THD is 2.1 % and 5.23 % for the SMC and ETSMC respectively.
Remark: Although, there is no band for the classical SMC, still the actual current chatters around the reference signal. this is because the SMC is not ideal.

3.5.2 ETSMC and Load variation

In this section, the adaptivity of the proposed scheme is discussed. To demonstrate the same, the current drawn from the grid is changed from 2.5 A to 5 A. The value of σ is kept as 0.07 for the study. As shown in Fig. 3.7, the band size adapts itself for the different current values so

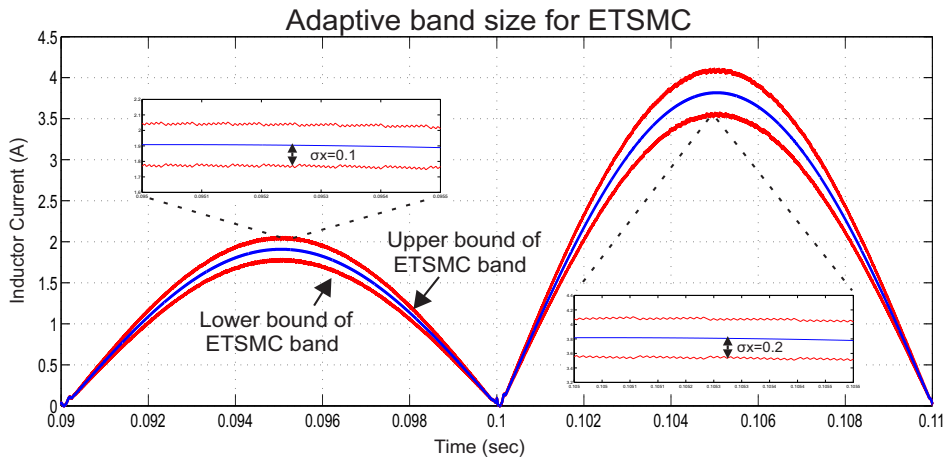

Figure 3.7 : Adaptive band for Event-triggered SMC for PFC

that the %THD can be maintained at a reduced switching. In this case the %THD is 4.87 % and 4.43 % for the two current values respectively. As the state changes so does the band, hence the sliding band is made adaptive by leveraging the state dynamics.
To establish the effectiveness of ETSMC over HM-SMC, system response to the similar load conditions for HM-SMC is provided below. The Fig 3.8 shows the reference current signal along with the allowable band around it for two different values of current. For HM-SMC control, here, the band stays of constant width through out. HM-SMC makes for a special case of ETSMC when the

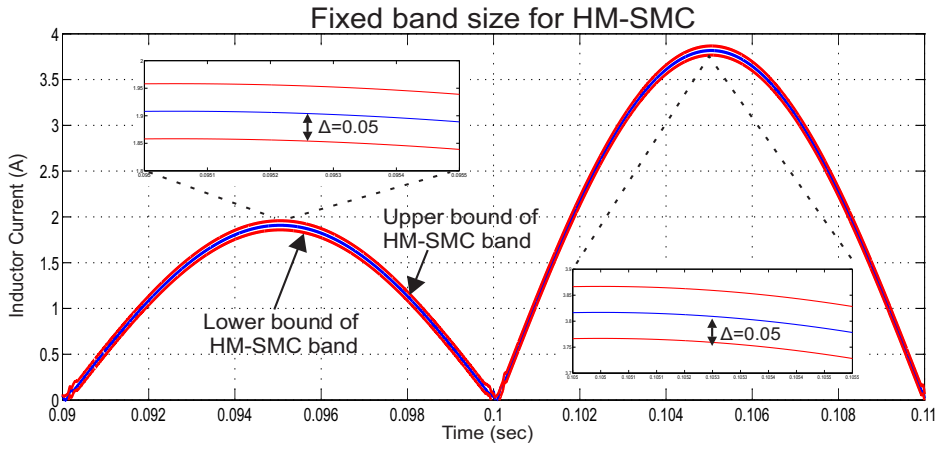

Figure 3.8 : Fixed band for HM-SMC

triggering condition is state independent, i.e. $||e|| \leq \sigma$. In order to correct the drawback of fixed

band size of HM-SMC, and further reduce the unnecessary switching an adaptive band is needed, which is exactly what the ETSMC proposes and has been discussed.

3.5.3 Experimental validation

The theoretical claims and simulation studies have been experimentally validated using a 200 W laboratory prototype of the converter. The designed converter, for the specifications provided in Table 3.3, and the set-up for the experimentation is shown in Fig. 3.9.

Table 3.3 : System Parameters

Parameter	Value
Boost converter	
Input Voltage Supply	100 V, 50 Hz
Nominal Output voltage	150 V
Inductance (L_o)	1.6 mH
Output capacitor (C_o)	220 μF

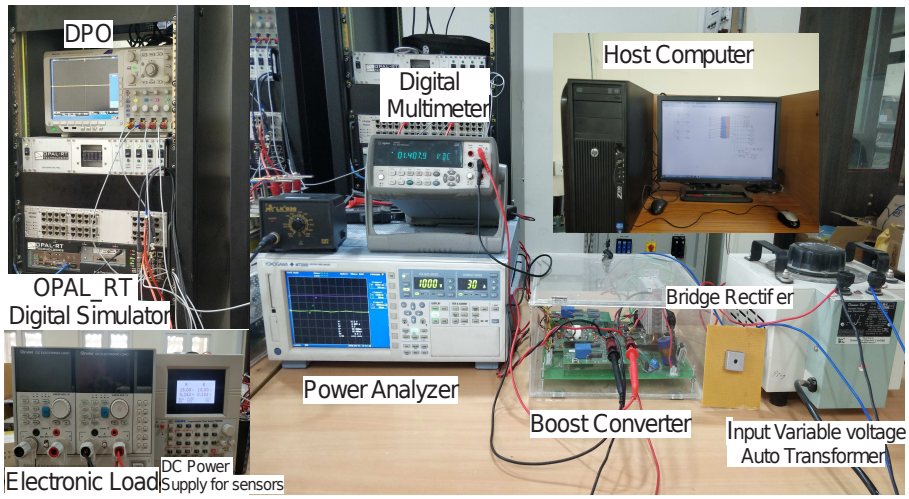

Figure 3.9 : Experimental setup

In Fig. 3.9, a boost converter, a bridge rectifier, electronic load, power analyser, digital multimeter, DC power supply for sensors, DPO and control platform (OPAL-Real Time Digital Simulator) are shown. The Isolation transformer takes power from the 230 V, 50 HZ mains and then on a variac is placed at the other end in order to vary the input ac voltage fed to the converter.

In order to highlight the performance of Event-triggered SLFR as compared to the Classical SLFR, the value of σ is changed from 0 to 0.2. When $\sigma = 0$, it implies that the triggering condition is always met, therefore, each instant is an event which is similar as the Classical SLFR implementation. The system response for the two cases has been presented in Fig. 3.10. The oscilloscope captures the Rectified AC voltage V_1, Inductor current I_L, and the corresponding switching pulses, under σ change. The channels have been set to 50 V/div for V_1, 100 mA/div for I_L and 25 V/div for the pulses. Time base is set to 40 ms/div.

As seen in Fig. 3.10, a reduction is seen in the switching pulse density for Event-triggered SLFR. Please note that, during this case the pulse density around $I_L = 0$ becomes same as Classical SLFR, as expected.

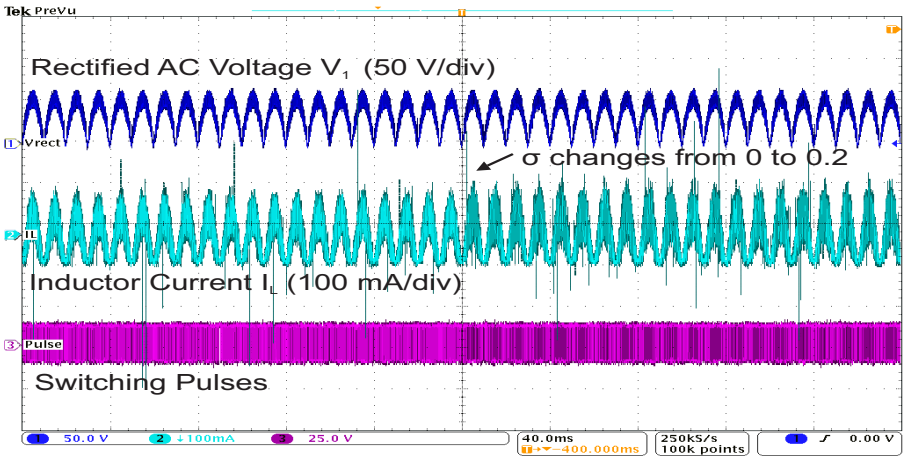

Figure 3.10 : Experimental validation. CH1: Rectified AC Input Voltage V_1 (50 V/div). CH2: Inductor Current I_L (100 mA/div). CH3: Switching Pulses

3.6 SUMMARY

In this Chapter, firstly, the need for power factor correction stage in household appliances is discussed, followed by the regulations imposed to keep the harmonic distortions in check. Then on, the concept of Sliding mode based LFR is discussed for PFC application. In light of the IEC 61000-3-2 guidelines, the need for load adaptive boundary conditions is demonstrated. The adopted strategy leverages system state to vary the band size thus serves as an ideal control scheme which eliminates unnecessary switching even while complying the regulatory standards. The expediency of the strategy has been shown over HM-SMC. The proposed theory is demonstrated and validated through simulation and experimentation.

The work presented in the Chapter, made use of SLFR for pre-regulator PFC application. Since the emulated SLFR stays fixed for all operating conditions, the strategy would not work for single stage PFC solutions. This motivated to propose an adaptive SLFR (ASLFR) in the next Chapter. The proposed ASLFR scheme gives a voltage regulation feature to the pre-regulator PFC, proposed using the existing SLFR technique, to accommodate any variations in the system parameters and still maintain the required performance.